




# A short review of phase transition in a chaotic system

Lucas K. A. Miranda<sup>1,a</sup> , Célia M. Kuwana<sup>1</sup>, Yoná H. Huggler<sup>1</sup>, Anne K. P. da Fonseca<sup>1</sup>, Makoto Yoshida<sup>1</sup>, Juliano A. de Oliveira<sup>1,2</sup>, and Edson D. Leonel<sup>1,b</sup>

<sup>1</sup> Departamento de Física, UNESP-Univ Estadual Paulista, Av.24A, 1515 Bela Vista, Rio Claro, SP 13506-900, Brazil

<sup>2</sup> UNESP-Univ Estadual Paulista, Câmpus de São João da Boa Vista, São João da Boa Vista, SP, Brazil

Received 16 June 2021 / Accepted 16 December 2021 / Published online 28 December 2021

© The Author(s), under exclusive licence to EDP Sciences, Springer-Verlag GmbH Germany, part of Springer Nature 2021

**Abstract** The subject approached here is a dynamical phase transition observed in Hamiltonian systems, which is a transition from integrability to non-integrability. Using the dynamics defined by a discrete mapping on the variables action  $I$  and angle  $\theta$ , we perform a description of the behaviour of the chaotic diffusion to particles in the chaotic sea using two methods. One is a phenomenological description obtaining the critical exponents via numerical simulation, and the other is an analytical result obtained by the solution of the diffusion equation. The scaling invariance is observed in the chaotic sea leading to a universal chaotic diffusion. This is a clear signature that the system is passing through a phase transition. We investigate a set of four questions that characterize a phase transition: (1) identify the broken symmetry; (2) define the order parameter; (3) identify what are the elementary excitations and; (4) detect the topological defects which impact on the transport of the particles.

## 1 Introduction

By the middle of XV and XVI centuries, after the initial investigations of dynamical systems, Isaac Newton, utilizing the formalism of mathematical laws and equations of motion, introduced the concept of a system evolving in time. In a dynamical system, by the knowledge of a configurational state (initial condition), it is possible to obtain any other state after that given the laws of the motion are known. In general such systems can be classified by linear and nonlinear systems [1]. The linear ones are mainly characterized by having first order powers in their dynamical equations. On the other hand, nonlinear systems are those that present power different of one in their equations, or those described by sine, cosine, exponential, among other non-linear functions.

In certain systems, such as fluids, density and viscosity, are control parameters that contribute to determine the intensity of nonlinear terms of their dynamical equations [1]. As we discuss in this review, modifying those parameters can lead the system to pass through a phase transition. Here we study a specific two-dimension mapping which nonlinearity is governed by the control parameter  $\epsilon$ . This parameter is responsible to rule a phase transition from integrability, where  $\epsilon = 0$ , to non-integrability with  $\epsilon$  different of zero, however, small and positive, so that characterising the transition. In addition, the phase space for  $\epsilon \neq 0$  is mixed,

presenting regular structures as periodic islands, which are surrounded by chaotic sea limited by the first invariant spanning curve. The diffusion of the particles in the chaotic sea is scaling invariant with respect to the control parameter, initial condition and time. Broken symmetry and scale invariance are remarkable signatures that the system is undergoing through a phase transition, in fact, a transition from integrability to non-integrability.

This review is organized as follows, in Sect. 2 we describe a generic Hamiltonian and enumerate different applications for a family of mappings. At Sect. 3 we identify the elliptic fixed points and the position of the first invariant spanning curve. In Sect. 4 it is approached a phenomenological description of particles diffusion in the chaotic sea, obtaining the critical exponents. An analytical description of this diffusion is provided in Sect. 5 via solution of the diffusion equation. In Sect. 6 we characterize the phase transition replaying the four proposed questions. Finally in Sect. 7 we present our final discussions and conclusions.

## 2 A family of Hamiltonian discrete mapping

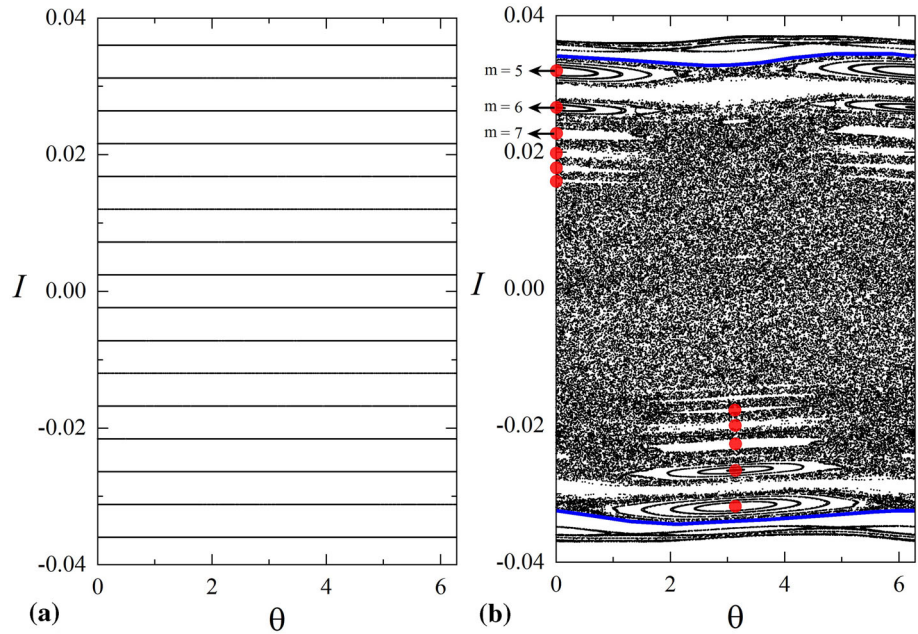
The dynamics of a system with two degrees of freedom can be described by a generic Hamiltonian as

$$H(I_1, \theta_1, I_2, \theta_2) = H_0(I_1, I_2) + \epsilon H_1(I_1, \theta_1, I_2, \theta_2). \quad (1)$$

<sup>a</sup> e-mail: [kenji.miranda@unesp.br](mailto:kenji.miranda@unesp.br) (corresponding author)

<sup>b</sup> e-mail: [edson-denis.leonel@unesp.br](mailto:edson-denis.leonel@unesp.br)

**Fig. 1** Phase space of the mapping (4) with  $\gamma = 1$  and: **a**  $\epsilon = 0$  and; **b**  $\epsilon = 10^{-3}$ . In **a** the phase space shows periodic and regular dynamics and is symmetric. In **b** the phase space becomes mixed, with the presence of the chaotic sea, periodic islands (centered by the elliptic fixed points marked in red bullets) and the first invariant spanning curves identified by the blue curves. The letter  $m$  characterizes the frequency of the sine function



Here, the integrable part is settled by  $H_0(I_1, I_2)$ , while the non-integrable part is given by  $H_1(I_1, \theta_1, I_2, \theta_2)$ , and  $\epsilon$  is a parameter that controls the transition from integrability ( $\epsilon = 0$ ) to non-integrability ( $\epsilon \neq 0$ ). The expression (1) gives us a four-dimensional flow of solutions. However, we can establish the energy of the system as a constant due to its time-independence [2, 3], thus we can eliminate one of the four variables. It is chosen  $I_2$ , remaining only a 3-D flow. Using a Poincaré section [4] to intercept this flow with a constant plane in  $\theta_2$ , we can reduce the 3-D flow to a 2-D mapping of  $I_1 \times \theta_1$ . This generic mapping can be written as [4]

$$\begin{cases} I_{n+1} = I_n + \epsilon h(\theta_n, I_{n+1}), \\ \theta_{n+1} = [\theta_n + K(I_{n+1}) + \epsilon p(\theta_n, I_{n+1})] \pmod{2\pi}, \end{cases} \quad (2)$$

where  $h(\theta_n, I_{n+1})$ ,  $K(I_{n+1})$  and  $p(\theta_n, I_{n+1})$  are nonlinear functions of their variables. Considering  $p(\theta_n, I_{n+1}) = 0$  and  $h(\theta_n, I_{n+1}) = \sin(\theta_n)$ , we obtain different dynamical systems well known in the literature, such as

- $K(I_{n+1}) = I_{n+1}$ , named the standard mapping [5–7];
- $K(I_{n+1}) = 2/I_{n+1}$ , which is the Fermi–Ulam model [8, 9];
- $K(I_{n+1}) = \zeta I_{n+1}$ , that describes the bouncer model [10], with  $\zeta$  as a constant;
- $K(I_{n+1}) = I_{n+1} + \zeta I_{n+1}^2$ , it is obtained the logistic twist mapping [11].

The index  $n$  (integer) indicates the iteration of the mapping. This generic mapping is area preserving only by the following condition:

$$\frac{\partial p(\theta_n, I_{n+1})}{\partial \theta_n} + \frac{\partial h(\theta_n, I_{n+1})}{\partial I_{n+1}} = 0. \quad (3)$$

For purpose of this review we consider  $h(\theta_n, I_{n+1}) = \sin(\theta_n)$ ;  $p(\theta_n, I_{n+1}) = 0$  and;  $K(I_{n+1}) = \frac{1}{|I_{n+1}|^\gamma}$ , with  $\gamma > 0$ . Therefore, the following mapping is obtained:

$$\begin{cases} I_{n+1} = I_n + \epsilon \sin(\theta_n) \\ \theta_{n+1} = \left[ \theta_n + \frac{1}{|I_{n+1}|^\gamma} \right] \pmod{2\pi} \end{cases} \quad (4)$$

The mapping has two control parameters. One is the parameter  $\epsilon$ , responsible to control the nonlinearity of the system. For  $\epsilon = 0$  the phase space has only regular and periodic structures, therefore, symmetric orbits, as shown in Fig. 1a. On the other hand, for  $\epsilon \neq 0$  the regularity is broken and the phase space becomes mixed, composed by chaotic sea, periodic islands and invariant spanning curves, as we see in Fig. 1b. The other parameter is  $\gamma > 0$ , which was chosen to control the velocity of the divergence of  $\theta$  in the limit that the action  $I$  is sufficiently small.

In fact, when  $I$  is small the term  $\theta_n + \frac{1}{|I_{n+1}|^\gamma}$  diverges, leading to uncorrelation between  $\theta_{n+1}$  and  $\theta_n$ . In this sense, the behaviour of  $\sin(\theta_n)$  becomes totally random, bringing chaotic orbits to the dynamics hence diffusion for the action variable. As the action  $I$  starts to grow, the angular variable begins to exhibit correlation, thus bringing regularity to the phase space, characterized by periodic islands and invariant curves.

### 3 Elliptic fixed points and the position of the first invariant spanning curve

#### 3.1 Elliptic fixed points

Observing Fig. 1b, we can notice the existence of a group of periodic islands. These islands are surrounded

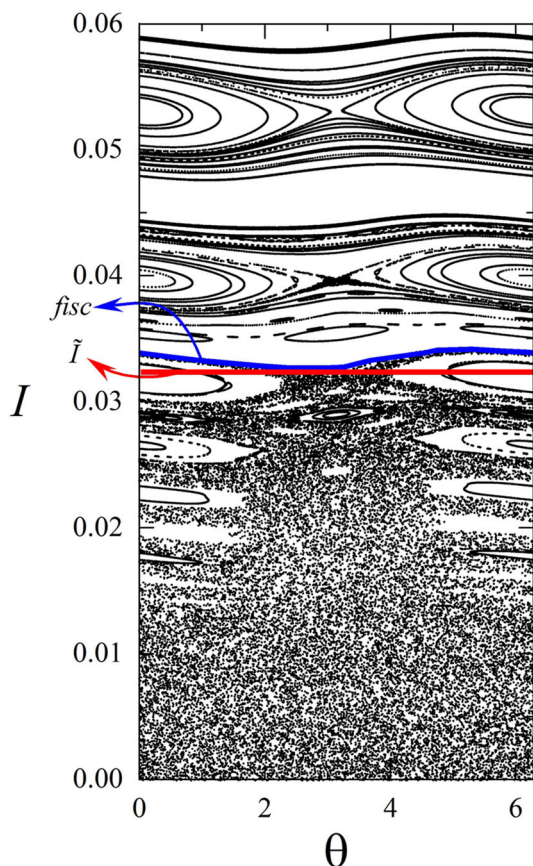


**Fig. 2** Plot of part of the phase space for  $\epsilon = 10^{-3}$  and a comparison of the analytical result obtained for the position of the first invariant spanning curve  $\tilde{I}$  (red curve) in (18), with the observational one, by the identification of broken structures (blue curve)

by the chaotic sea, which is limited by the first invariant spanning curves. Once an orbit starts to grow in the chaotic sea, it cannot get in the periodic islands, nor pass through the invariant spanning curves at the price of violating the Liouville’s theorem.

The fixed points can be obtained by the following conditions: [1, 12, 13]

$$\begin{aligned} I_{n+1} &= I_n = I^*, \\ \theta_{n+1} &= \theta_n = \theta^* + 2m\pi, \quad m = 1, 2, 3, \dots \end{aligned} \tag{5}$$

Substituting Eq. (5) into Eq. (4), we end up with

$$(\theta^*, I^*) = \left\{ 0, \pm \left(\frac{1}{2m\pi}\right)^{\frac{1}{\gamma}}, \pi, \pm \left(\frac{1}{2m\pi}\right)^{\frac{1}{\gamma}} \right\}, \tag{6}$$

where  $(\theta^*, I^*)$  are the coordinates for the elliptic fixed points. Figure 1b shows some of them for  $m = 5, 6$  and  $7$  in well agreement to Eq. (6).

### 3.2 Invariant spanning curves

The chaotic sea is limited by the first invariant spanning curves. They prevent a chaotic orbit to diffuse unbounded. The lowest one determine the transition from a local chaos (above the curve) to a global one (below the curve).

As shown in Fig. 2, it is noticed that considering  $\epsilon = 10^{-3}$  and for  $I \gg \epsilon$ , the fluctuations of the invariant spanning curves are too small compared on to the size of the chaotic sea. Therefore, we assume [14, 15] that in its vicinity, the dynamics of the action  $I$  can be given by

$$I_n = \tilde{I} + \Delta I_n, \tag{7}$$

consequently

$$I_{n+1} = \tilde{I} + \Delta I_{n+1}, \tag{8}$$

where  $\tilde{I}$  corresponds to a characteristic value of  $I$  along the invariant spanning curve, and  $\Delta I_n$  is a small perturbation upon  $\tilde{I}$ . It is important to emphasize that this theoretical approximation is only suitable for small values of  $\epsilon$ , i.e. near the transition from integrability ( $\epsilon = 0$ ) to non-integrability ( $\epsilon \neq 0$ ), otherwise that approximation is no longer eligible.

Using the result (8), the first equation of the mapping (4) can be written as

$$\Delta I_{n+1} = \Delta I_n + \epsilon \sin(\theta_n). \tag{9}$$

Considering this approximation for the second equation of the mapping (4) we have

$$\theta_{n+1} = \theta_n + \frac{1}{\tilde{I}^\gamma} \left[ 1 + \frac{\Delta I_{n+1}}{\tilde{I}} \right]^{-\gamma}. \tag{10}$$

Implementing a Taylor expansion in Eq. (10), around  $\frac{\Delta I_{n+1}}{\tilde{I}} = 0$  (Maclaurin series), we obtain

$$\theta_{n+1} = \theta_n + \frac{1}{\tilde{I}^\gamma} - \frac{\gamma \Delta I_{n+1}}{\tilde{I}^{\gamma+1}}. \tag{11}$$

Now, to establish a connection with the standard mapping, Eq. (9) is multiplied by  $\frac{-\gamma}{\tilde{I}^{\gamma+1}}$ , thus

$$-\frac{\gamma \Delta I_{n+1}}{\tilde{I}^{\gamma+1}} = -\frac{\gamma \Delta I_n}{\tilde{I}^{\gamma+1}} - \frac{\gamma \epsilon \sin \theta_n}{\tilde{I}^{\gamma+1}}, \tag{12}$$

and then added the term  $1/\tilde{I}^\gamma$ , so that we end up with

$$\frac{1}{\tilde{I}^\gamma} - \frac{\gamma \Delta I_{n+1}}{\tilde{I}^{\gamma+1}} = \frac{1}{\tilde{I}^\gamma} - \frac{\gamma \Delta I_n}{\tilde{I}^{\gamma+1}} - \frac{\gamma \epsilon \sin \theta_n}{\tilde{I}^{\gamma+1}}. \tag{13}$$

By convenience, we also define the following variables:

$$J_{n+1} = \frac{1}{\tilde{I}^\gamma} - \frac{\gamma \Delta I_{n+1}}{\tilde{I}^{\gamma+1}}, \tag{14}$$

$$\phi_n = \theta_n + \pi. \tag{15}$$

Thus, using the conditions defined in (14) and (15) on the Eqs. (13) and (11), we can rewrite the initial mapping (4) as

$$\begin{cases} J_{n+1} = J_n + \frac{\gamma \epsilon_n}{\tilde{I}^{\gamma+1}} \sin(\phi_n), \\ \phi_{n+1} = \phi_n + J_{n+1}, \end{cases} \quad (16)$$

therefore, the dynamics of the mapping (4) near the invariant spanning curve is described by the standard mapping. In addition, an effective control parameter is identify, which is

$$K_{ef} = \frac{\gamma \epsilon}{\tilde{I}^{\gamma+1}}. \quad (17)$$

As discussed in Refs. [4, 5, 16], near the transition from local to global chaos (i.e. near the first invariant spanning curve)  $K_{ef} \simeq 0.9716\dots$ , hence the estimated position for the first invariant spanning curve  $\tilde{I}$  is given by

$$\begin{aligned} \tilde{I} &= \left[ \frac{\gamma \epsilon}{0.9716} \right]^{\frac{1}{\gamma+1}}, \\ &= \left[ \frac{\gamma}{0.9716} \right]^{\frac{1}{\gamma+1}} \epsilon^{\frac{1}{1+\gamma}}. \end{aligned} \quad (18)$$

Figure 2 shows that the analytical result  $\tilde{I}$  of Eq. (18) is in well agreement compared to the first invariant spanning curve (*fsic*) observed in the phase space of the mapping (4) for the parameters  $\epsilon = 10^{-3}$  and  $\gamma = 1$ .

### 4 A phenomenological description of particles diffusion and the critical exponents

As seen in the phase space, the chaotic sea is limited by the invariant spanning curves. It allows the particle to diffuse along the action axis. To characterize the scaling properties of the average action, i.e., the particles diffusion in the chaotic sea, we use the same procedure of Refs. [1, 14, 15], once the formalism has already been applied to many other systems and mappings with great success [17–26].

It is used the variable  $\overline{I^2}$  as the observable, since  $\overline{I} = 0$  is not a good observable due to the symmetry between the upper part (positive) and the bottom part (negative) of the phase space. The chosen observable defines the root-mean-square of the action  $I_{rms} = \sqrt{\overline{I^2}}$  (see Refs. [27, 28]). This last one can be given by two averages

$$I_{rms} = \sqrt{\frac{1}{M} \sum_{i=1}^M \left[ \frac{1}{n} \sum_{j=1}^n I_{i,j}^2 \right]}. \quad (19)$$

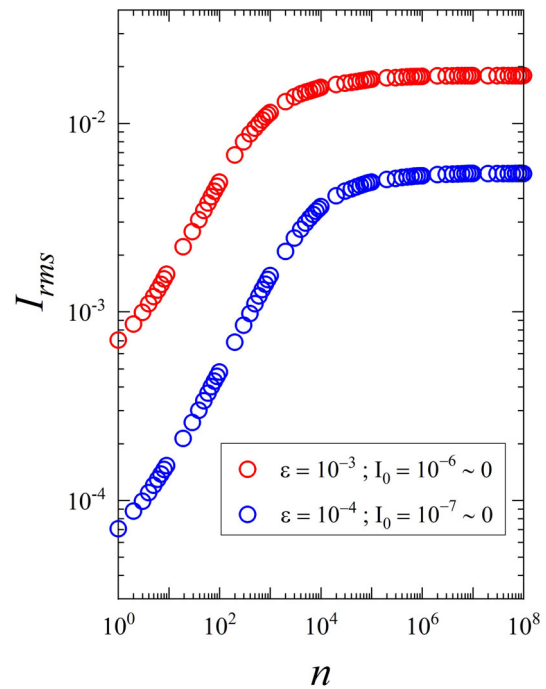


**Fig. 3** Plot of  $I_{rms}$  vs.  $n$  for two different control parameters  $\epsilon$  and  $\gamma = 1$

Here,  $M$  corresponds to the number of initial conditions, and  $n$  characterizes the number of iterations of the mapping. The summation in  $i$  identifies the average over the ensemble of initial conditions, whereas the summation in  $j$  corresponds to an average over the orbit produced by the mapping iteration.

Figure 3 shows the behaviour of  $I_{rms}$  vs.  $n$  for  $\gamma = 1$  and two different control parameters  $\epsilon$ . We used  $M = 1000$  initial values of the angle  $\theta_0 \in [0, 2\pi]$ , which were chosen uniformly distributed for a fixed initial value  $I_0 = 10^{-3}\epsilon$ . For short times of the iteration ( $n \ll n_x$ ) the curves present an accelerated growth regime. On the other hand, for long enough time ( $n \gg n_x$ ), the curves achieve a limit of saturation, marked by a constant plateau. The transition from the first rule of growth to a regime of constant saturation is given by a characteristic value  $n_x$ , which is the crossover number.

These three behaviours presented by the curves of  $I_{rms}$  as a function of time  $n$  can be characterized by three critical exponents ( $\alpha, \beta$  and  $z$ ). To obtain these three exponents we assume the following scaling hypotheses [14, 15]:

1. For values of  $n \ll n_x$ , the behaviour of  $I_{rms}$  is given by

$$I_{rms} \propto (n\epsilon^2)^\beta, \quad (20)$$

where  $\beta$  identifies the acceleration exponent.

2. For  $n \gg n_x$ , the curves archive a saturation regime, which can be described by

$$I_{rms,sat} \propto \epsilon^\alpha, \quad (21)$$

where  $\alpha$  is the saturation exponent.

- Finally, we have the changeover from an accelerated regime of growth to a constant plateau, identified by the crossover number  $n_x$ :

$$n_x \propto \epsilon^z, \tag{22}$$

where  $z$  is the crossover exponent.

Therefore, using those three scaling hypotheses, we can describe the behaviour of  $I_{rms}$  by a generalized homogeneous function, which is given by

$$I_{rms}(n\epsilon^2, \epsilon) = l I_{rms}(l^a n\epsilon^2, l^b \epsilon), \tag{23}$$

where  $l$  is a scaling factor,  $a$  and  $b$  are characteristic exponents. First, it is convenient to choose that  $l^a n\epsilon^2 = 1$ , so we have

$$l = (n\epsilon^2)^{-\frac{1}{a}}. \tag{24}$$

Bringing Eq. (24) to Eq. (23), we end up with

$$I_{rms}(n\epsilon^2, \epsilon) = (n\epsilon^2)^{-\frac{1}{a}} I_{rms}(1, (n\epsilon^2)^{-\frac{b}{a}} \epsilon), \tag{25}$$

wherein  $I_{rms}(1, (n\epsilon^2)^{-\frac{b}{a}} \epsilon)$  is assumed to be a constant for  $n \ll n_x$ , thus comparing Eq. (25) with the first scaling hypothesis (20) we have that  $(n\epsilon^2)^{-\frac{1}{a}} = (n\epsilon^2)^\beta$  which leads us to  $\beta = -1/a$ .

Performing this same procedure, however, for  $l^b \epsilon = 1$ , we obtain

$$l = \epsilon^{-\frac{1}{b}}. \tag{26}$$

Now, using Eq. (26), Eq. (23) can be rewritten as

$$I_{rms}(n\epsilon^2, \epsilon) = \epsilon^{-\frac{1}{b}} I_{rms}(\epsilon^{-\frac{a}{b}} n\epsilon^2, 1), \tag{27}$$

where  $I_{rms}(\epsilon^{-\frac{a}{b}} n\epsilon^2, 1)$  is considered a constant for values of  $n \gg n_x$  (saturation regime). Therefore, making a comparison between Eq. (27) and the second scaling hypothesis (21), we have  $\epsilon^\alpha = \epsilon^{-\frac{1}{b}}$  that results in  $\alpha = -1/b$ .

The critical exponent  $z$  can be obtained by combining the two scaling factors (24), (26), and using  $\alpha = -1/b$  and  $\beta = -1/a$  leading us to

$$(n\epsilon^2)^\beta = \epsilon^\alpha \implies \boxed{n_x = \epsilon^{\frac{\alpha}{\beta} - 2}}. \tag{28}$$

Finally, comparing the framed Eq. (28) with the third scaling hypothesis (22), we obtain

$$\underbrace{z = \frac{\alpha}{\beta} - 2}_{\text{Scaling law}}. \tag{29}$$

Equation (29) gives us an analytical expression with the three critical exponents, therefore, defining a scaling

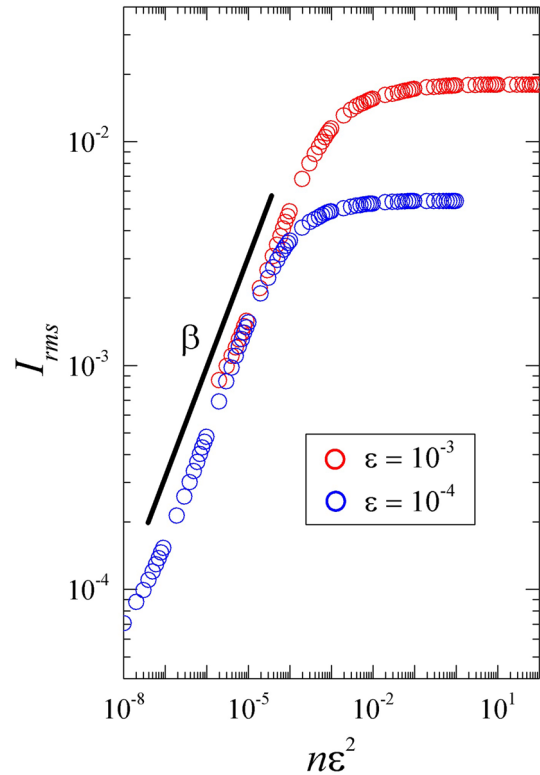


**Fig. 4** Same plot of Fig. 3 after the transformation  $n \rightarrow n\epsilon^2$ . The value obtained for the critical exponent is  $\beta = 0.501(5)$

law. In fact, by the knowledge of two critical exponents, we can also find the third one.

By numerical simulation, we were able to obtain the critical exponent  $\beta$  from a power law fitting. To do so, we used the transformation that correlates the regime of growth as in the first scaling hypothesis (20), hence we have  $n \rightarrow n\epsilon^2$ . Figure 4 shows the same plot of Fig. 3 after this transformation. The numerical value obtained was  $\beta = 0.501(5)$ .

The exponent  $\alpha$  was obtained using the relation established by the second scaling hypothesis (21), so that for long enough  $n$  the constant regime of saturation relates  $I_{rms,sat} \propto \epsilon^\alpha$ . Therefore, we plotted the behaviour of  $I_{rms,sat}$  for different values of the control parameter  $\epsilon$ . The value obtained for the critical exponent due to the power law fitting is  $\alpha = 0.515(6)$ , as shown in Fig. 5.

Finally, we have the critical exponent  $z$ , which is defined by the third scaling hypothesis (22). The crossover number  $n_x$ , that marks the transition from a growth regime to a constant plateau of saturation, is obtained when we plot  $n_x$  vs.  $\epsilon$  to obtain the critical exponent  $z$ . Figure 6 shows a power law fitting that gives us  $z = -0.97(2)$ .

It is important to notice that the result obtained for  $z$  by the simulational method is in well agreement with the scaling law proposed by Eq. (29). In addition, the critical exponents obtained confirm the scaling invariance found in the chaotic sea of the phase space. To do

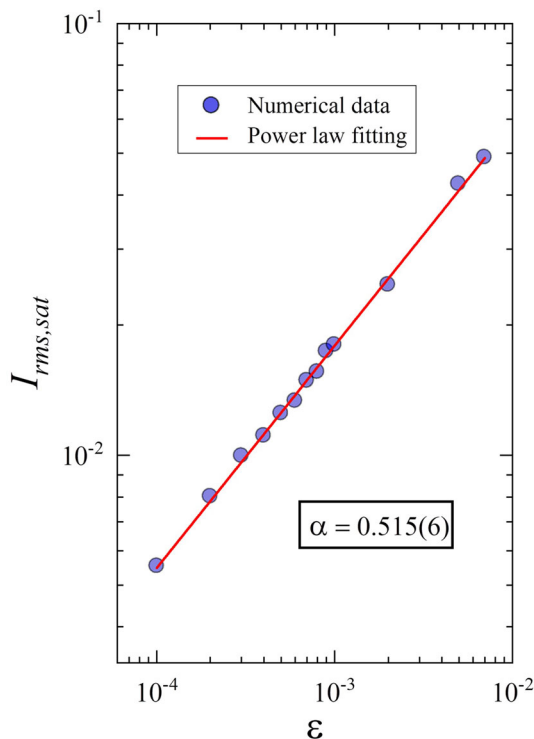


**Fig. 5** Plot of  $I_{rms,sat}$  vs.  $\epsilon$  for  $n \gg n_x$ , using  $\gamma = 1$ . The critical exponent obtained was  $\alpha = 0.515(6)$

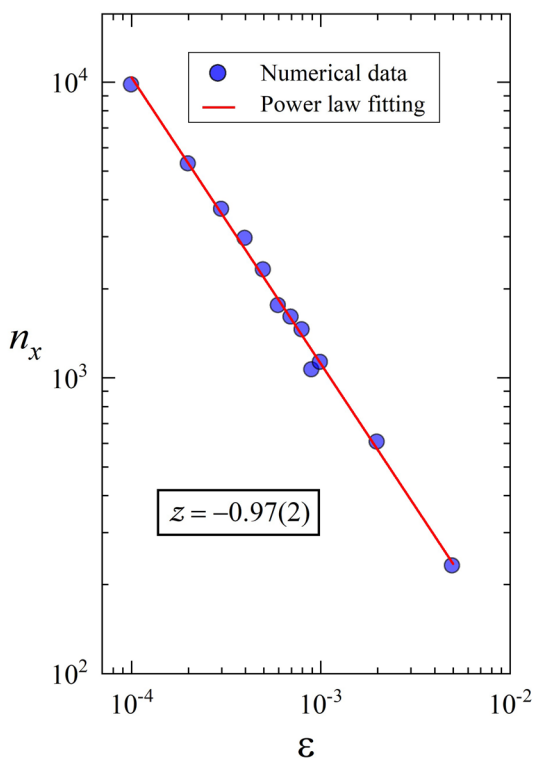


**Fig. 6** Behaviour of  $n_x$  vs.  $\epsilon$ , using  $\gamma = 1$ . The critical exponent obtained was  $z = -0.97(2)$

so, we overlap the curves of  $I_{rms}$  vs.  $n$  for different  $\epsilon$  into a single and universal curve. The transformation to be done is  $I_{rms} \rightarrow I_{rms}/\epsilon^\alpha$  and  $n \rightarrow n/\epsilon^z$ .

Figure 7a shows the plot of  $I_{rms}$  vs.  $n$  for five different control parameters  $\epsilon$ , while Fig 7b displays all the curves plotted in (a) overlapped onto an universal curve after the mentioned transformation.

### 5 An analytical description of particles diffusion via solution of the diffusion equation

In this section we describe analytically the behaviour of particle diffusion in the chaotic sea given in the phase space through the solution of the diffusion equation. To do so, we use the same formalism performed in Ref. [29] we need to find  $P(I, n)$ , which is the probability to observe an action  $I$  in an instant of time  $n$ . Therefore, we use the well-known diffusion equation [30], which is written as

$$\frac{\partial P(I, n)}{\partial n} = D \frac{\partial^2 P(I, n)}{\partial I^2}, \tag{30}$$

where  $P$  is the required probability and  $D$  is the diffusion coefficient.

As mentioned before, the chaotic sea is limited by the first invariant spanning curve, thus the chaos diffuses with a range  $I_{chaos} \in [-I_{fisc}, +I_{fisc}]$ , as we can see in Fig. 8. We also know that an initial condition given along these curves stays trapped onto them for any time  $n \geq 0$ . Therefore, we have the following boundary condition:

$$\left. \frac{\partial P(I, n)}{\partial I} \right|_{I=\pm I_{fisc}} = 0. \tag{31}$$

The initial conditions are chosen in a way that all of them are centered at  $I = I_0$  and  $n = 0$ , thus

$$P(I_0, n) = \delta(I - I_0), \tag{32}$$

where  $\delta(I - I_0)$  is the Dirac delta function.

First, we find the diffusion coefficient  $D$ , which can be given by  $\overline{\Delta I^2}/2$ . Therefore, using the mean square of the first equation of the mapping (4), and knowing that  $\sin^2 \theta_n = 1/2$ , we have that

$$D = \frac{\overline{I_{n+1}^2} - \overline{I_n^2}}{2} = \frac{\epsilon^2}{4}. \tag{33}$$

To solve the diffusion equation the process used here is the separation of variables method [30], so it is defined

$$P(I, n) = X(I)Y(n), \tag{34}$$

**Fig. 7** **a** Same plot of Fig. 3 for five different control parameters  $\epsilon$  and  $\gamma = 1$ . **b** Overlap of all the curves plotted in **a** onto a single and universal one after the transformation  $I_{rms} \rightarrow I_{rms}/\epsilon^\alpha$  and  $n \rightarrow n/\epsilon^z$

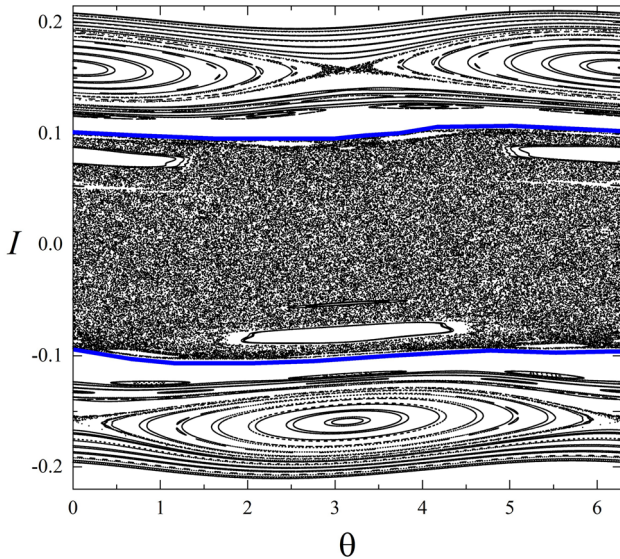
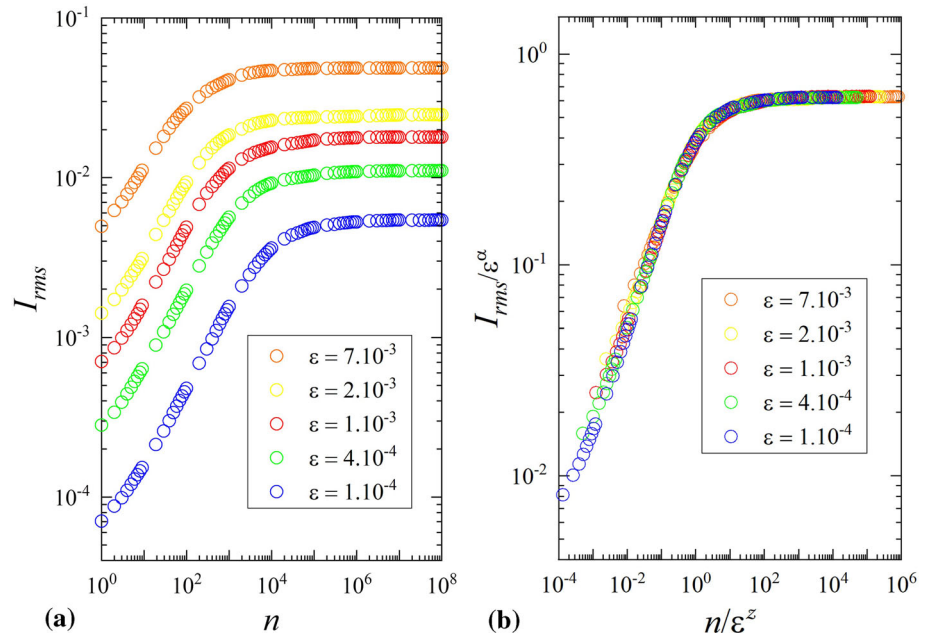


**Fig. 8** Phase space of the mapping (4) for  $\gamma = 1$  and  $\epsilon = 10^{-2}$ . The blue curves represent the first invariant spanning curve

where  $X(I)$  and  $Y(n)$  are any functions that depend only on  $I$  and  $n$ , respectively. Rearranging Eq. (30), we obtain

$$\frac{1}{Y(n)} \frac{\partial Y(n)}{\partial n} = \frac{D}{X(I)} \frac{\partial^2 X(I)}{\partial I^2} = -\lambda, \quad \text{with } \lambda \in \mathbb{R}^+ \tag{35}$$

The solutions for  $X(I)$  and  $Y(n)$  of Eq. (35) are given by

$$X(I) = 2A \cos\left(\sqrt{\frac{\lambda}{D}} I\right), \tag{36}$$

$$Y(n) = Y_0 e^{-\lambda n}. \tag{37}$$

Hence, a solution of  $P(I, n)$  can be written as

$$P(I, n) = 2A \cos\left(\sqrt{\frac{\lambda}{D}} I\right) Y_0 e^{-\lambda n}. \tag{38}$$

Applying the initial conditions of  $I = I_0$  and  $n = 0$ , we obtain

$$\tilde{C}_0 = 2A \cos\left(\sqrt{\frac{\lambda}{D}} I_0\right) Y_0. \tag{39}$$

Now, using the boundary condition established on (31), we obtain

$$\left. \frac{\partial P(I, n)}{\partial I} \right|_{I=\pm I_{fisc}} = -2A \sqrt{\frac{\lambda}{D}} \sin\left(\sqrt{\frac{\lambda}{D}} I_{fisc}\right) Y_0 e^{-\lambda n}, \tag{40}$$

which is null for values of  $\sqrt{\frac{\lambda}{D}} I_{fisc} = k\pi$ , with  $k = 1, 2, 3 \dots$ . Therefore, we have that

$$\lambda = \frac{k^2 \pi^2}{I_{fisc}^2} D. \tag{41}$$

Noticing that the specific case of  $k = 0$  we have  $\lambda = 0$ . Thus, new solutions are obtained for  $X(I)$  and  $Y(n)$  of Eq. (35), and consequently a new solution for  $P(I, n)$  can be given by

$$P(I, n) = \tilde{Y}_0 (X_0 + cI), \tag{42}$$

where  $\tilde{Y}_0$ ,  $X_0$  and  $c$  are constants.

Using again the boundary condition (31), we obtain  $c = 0$ ; therefore, we can write a general solution of  $P(I, n)$  as

$$P(I, n) = C_0 + \sum_{k=1}^{\infty} C_k \cos \left[ \frac{k\pi I}{I_{\text{fisc}}} \right] e^{-\frac{k^2 \pi^2 D}{I_{\text{fisc}}^2} n}, \quad (43)$$

here  $C_0 = \tilde{Y}_0 X_0 + \tilde{C}_0$  and  $C_k = 2AY_0$ , which are coefficients to be obtained.

These coefficients can be acquired using simple integrals and the probability normalization  $\int_{-I_{\text{fisc}}}^{+I_{\text{fisc}}} P(I, n) dI = 1$  (see Ref. [31] for more details), which leads us to

$$C_0 = \frac{1}{2I_{\text{fisc}}}, \quad (44)$$

$$C_k = \frac{1}{I_{\text{fisc}}}. \quad (45)$$

Therefore, rewriting Eq. (43), we end up with

$$P(I, n) = \frac{1}{2I_{\text{fisc}}} + \frac{1}{I_{\text{fisc}}} \sum_{k=1}^{\infty} \cos \left[ \frac{k\pi I}{I_{\text{fisc}}} \right] e^{-\frac{k^2 \pi^2 D}{I_{\text{fisc}}^2} n}. \quad (46)$$

We also use  $\bar{I}^2$  as the observable, since  $\bar{I} = 0$  is not a good choice because of the phase space symmetry. The average over the ensemble of initial conditions via solution of the diffusion equation is given by  $\bar{I}^2(n) = \int_{-I_{\text{fisc}}}^{+I_{\text{fisc}}} I^2 P(I, n) dI$ , which gives us

$$\bar{I}^2(n) = I_{\text{fisc}}^2 \left[ \frac{1}{3} + \frac{4}{\pi^2} \sum_{k=1}^{\infty} \frac{(-1)^k}{k^2} e^{-\frac{k^2 \pi^2 D}{I_{\text{fisc}}^2} n} \right]. \quad (47)$$

Notice that in the same way of the phenomenological description, we had two averages, one regarding the ensemble of initial conditions, as described by Eq. (47), and the other one was a average over all the orbits produced by the iteration of the mapping. Therefore, to consider this second average we define  $\bar{I}^{2*}(n) = \frac{1}{n} \sum_{j=1}^n \bar{I}_j^2$ . As we can see in Eq. (47), only the last term depends on  $n$ , what leads us to write

$$\begin{aligned} \frac{1}{n} \sum_{j=1}^n e^{-\frac{k^2 \pi^2 D}{I_{\text{fisc}}^2} j} &= \frac{1}{n} \left[ e^{-\frac{k^2 \pi^2 D}{I_{\text{fisc}}^2}} + e^{-\frac{k^2 \pi^2 D}{I_{\text{fisc}}^2} 2} + \dots + e^{-\frac{k^2 \pi^2 D}{I_{\text{fisc}}^2} n} \right], \\ &= \frac{1}{n} \left[ e^{-\frac{k^2 \pi^2 D}{I_{\text{fisc}}^2}} \left( \frac{1 - e^{-\frac{k^2 \pi^2 D}{I_{\text{fisc}}^2} n}}{1 - e^{-\frac{k^2 \pi^2 D}{I_{\text{fisc}}^2}}} \right) \right]. \end{aligned} \quad (48)$$

Using Eq. (48) we can finally obtain the behaviour of  $I_{\text{rms}} = \sqrt{\bar{I}^{2*}(n)}$  analytically, thus we end up with

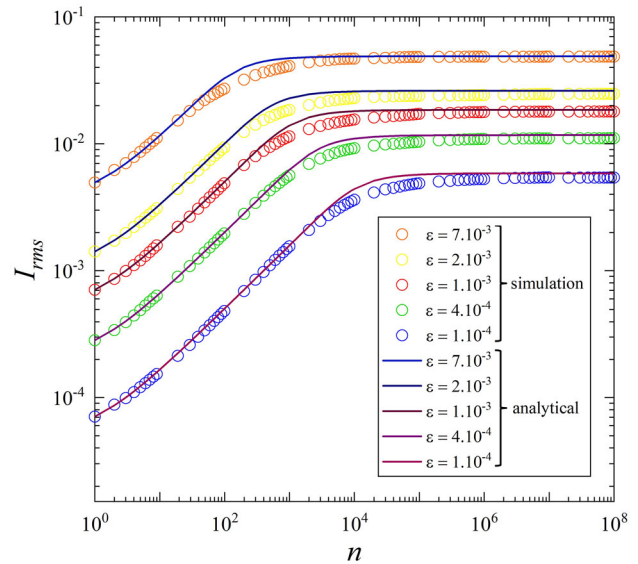


**Fig. 9** Plot of  $I_{\text{rms}}$  vs.  $n$  with  $\gamma = 1$  and five different values of  $\epsilon$ . The circles represent a phenomenological description of  $I_{\text{rms}}$ . On the other hand, the continuous lines represent the same observable, however, for a analytical description via solution of the diffusion equation

$$I_{\text{rms}} = I_{\text{fisc}} \sqrt{\frac{1}{3} + \frac{4}{\pi^2} \sum_{k=1}^{\infty} \frac{(-1)^k}{k^2} \frac{1}{n} \left[ e^{-\frac{k^2 \pi^2 D}{I_{\text{fisc}}^2}} \left( \frac{1 - e^{-\frac{k^2 \pi^2 D}{I_{\text{fisc}}^2} n}}{1 - e^{-\frac{k^2 \pi^2 D}{I_{\text{fisc}}^2}}} \right) \right]}. \quad (49)$$

Equation (49) describes analytically the behaviour of particles diffusion present in the chaotic sea of the phase space.

Figure 9 shows a plot of  $I_{\text{rms}}$  vs.  $n$  with  $\gamma = 1$  and five different control parameters  $\epsilon$  comparing the two methods used in this review to describe this observable. The circles represent the numerical simulation obtained in Sect. 4, and the continuous line refers to the analytical result obtained through the solution of the diffusion equation.

## 6 An insight on the phase transition

### 6.1 Broken symmetry

This first topic can be analyzed observing the results presented in the beginning of this review at Sect. 2. This one refers to the broken symmetry of the phase space. Since the modification in the control parameter from  $\epsilon = 0$  (integrable system) to  $\epsilon = 10^{-3}$  (non-integrable), the phase space that presented symmetrical and regular curves in Fig 1a turns into a mixed phase space with



well defined structures at Fig 1b, composed by periodic islands surrounded for the chaotic sea, and this last one limited by invariant spanning curves. Therefore, it is identified the broken symmetry of the system duo to a modification in the control parameter near the transition from integrability to non-integrability.

### 6.2 Order parameter

As shown in Ref. [27], the order parameter can be characterized by the important variable that describes the dynamics of a system. In this sense, we noticed that a candidate to be an order parameter is  $I_{\text{rms,sat}}$ .

Before checking this choice, first, we can rewrite the second scaling hypothesis (21) in Sect. 4 using the result of  $\tilde{I}$  in Eq.(18) of Sect. 3.1. This is possible, because, as discussed in Ref. [14], the location of the lowest invariant spanning curve delimits a transition from a local chaos, above this curve, to a global one in the chaotic sea. Therefore, the behaviour of the particles diffusion  $I_{\text{rms}}$  must be linked with  $\tilde{I}$  for  $n \gg n_x$ . Hence, comparing Eq. (18) with Eq. (21) we find that

$$\alpha = \frac{1}{1 + \gamma} \quad \gamma > 0 \tag{50}$$

so that the second scaling hypothesis can be rewritten as  $I_{\text{rms,sat}} \propto \epsilon^{\frac{1}{\gamma+1}}$ .

We can notice by the second scaling hypothesis  $I_{\text{rms,sat}} \propto \epsilon^{\frac{1}{\gamma+1}}$  and by Fig. 5, as soon the control parameter  $\epsilon \rightarrow 0$ , the order parameter chosen  $I_{\text{rms,sat}}$  approaches to zero continuously. In addition, the second condition can be evaluated in the following manner:

$$\chi = \left. \frac{\partial I_{\text{rms,sat}}}{\partial \epsilon} \right|_{\epsilon \rightarrow 0}$$

which gives us

$$\begin{aligned} \chi &= \lim_{\epsilon \rightarrow 0} \left[ \frac{1}{\gamma + 1} \right] \epsilon^{\frac{1}{\gamma+1}-1}, \\ &= \lim_{\epsilon \rightarrow 0} \left[ \frac{1}{\gamma + 1} \right] \frac{1}{\epsilon^{\frac{\gamma}{\gamma+1}}}. \end{aligned} \tag{51}$$

Here,  $\chi$  gives how is the behaviour of the response of the order parameter due to the variation of the control parameter. As we defined  $\gamma > 0$ , so in the limit of  $\epsilon \rightarrow 0$  we have that  $\chi \rightarrow \infty$ . This is a clear signature that the phase transition we are facing is a second-order phase transition (continuous phase transition).

### 6.3 Elementary excitations

To investigate the elementary excitations we must remember some properties about the mapping (4). It was observed the presence of two control parameters. One of them is  $\epsilon$ , which controls the intensity of non-linearity of the system given by the nonlinear term

$\sin(\theta_n)$ . The other one is  $\gamma > 0$ , this parameter is responsible to control the divergence of the angle  $\theta$  in a limit of small action  $I$ . In fact, it was noticed that when  $I$  is sufficiently small, the term  $\theta_n + \frac{1}{|I_{n+1}|^\gamma}$  diverges, existing no correlation between  $\theta_{n+1}$  and  $\theta_n$ . Therefore, the behaviour of  $\sin(\theta_n)$  becomes totally random, as the well-known random walk problem [27, 28]. That brings a diffusion of chaotic orbits into the phase space, as shown in Fig. 1b. As soon the angular variable starts to present correlation due to the increase of the action  $I$ , regular orbits begin to appear in the phase space, as periodic islands and invariant curves.

The amplitude  $I_a$  of this random behaviour can be obtained by taking the root-mean-square of the first equation of the mapping (4). In addition, we considered that the initial conditions established to the system are close to zero, so that  $\overline{I_n^2} \simeq 0$ , therefore, we have

$$\overline{I_{n+1}^2} = \overline{I_n^2} + \epsilon^2 \overline{\sin^2(\theta_n)}, \tag{52}$$

that leads us to

$$I_a = \frac{\epsilon}{\sqrt{2}}, \tag{53}$$

since  $\overline{\sin^2 \theta_n} = 1/2$ . Therefore, here, we identify that the elementary excitations of this system are defined by the nonlinear function  $\epsilon \sin(\theta_n)$  of the first equation of the mapping (4), which amplitude is given by  $I_a = \epsilon/\sqrt{2}$ . This term leads to a totally random dynamics in the limit of small values of  $I$ , thus bringing chaotic orbits to the phase space.

### 6.4 Topological defects

The topological defects are totally related to the probability of the particles distribution over the phase space. The periodic islands, centered by an elliptic fixed point, are the main structures responsible for these defects. This fact is given by the loss of predictability about the dynamics of the system. That occurs due to the stickiness effect [32], which is characterized by a temporary trapping over the chaotic orbits near those regular structures (islands of stability). This effect leads to a more dense distribution of particles in such areas, therefore, destroying the ergodicity [27] in the dynamics.

We also can analyze the survival probability  $\rho$ , which defines the probability of a particle to survive over a chaotic dynamics without escaping this region. As seen in [33], it was noticed a relevant modification in this probability as a result of the stickiness effect, which was the transition from an exponential decay of  $\rho$  along of the time  $n$ , to a slower one in power law. The exponential decay of this probability defines the dynamics which particles transport of the system is normal (Brownian diffusion). On the other hand, this change to a slower decay in power law characterizes the presence of the stickiness effect, where the chaotic orbits remain temporarily trapped near those periodic islands. Therefore,

the periodic islands are identified as the topological defects that impact on the particles diffusion.

## 7 Conclusions and discussion

In this review, using the dynamics of a discrete mapping on the variables action  $I$  and angle  $\theta$ , it is characterized a dynamical phase transition from integrability to non-integrability, which is controlled by the parameter  $\epsilon$ . At the beginning of this description we focused on defining some properties of the characteristic mixed phase space. We identify the elliptic fixed points and locate the first invariant spanning curve, that determines a transition from a local chaos (above the curve) to a global one (below the curve). Latter, using two different methodologies, we perform a characterization of the particles diffusion in the chaotic sea of the phase space. First we resort to a phenomenological description, using a simulational process. Analyzing the curves of  $I_{rms}$  vs.  $n$  and assuming three scaling hypotheses we were capable to define a scaling law that correlates the three critical exponents  $\alpha$  (saturation exponent),  $\beta$  (acceleration exponent) and  $z$  (crossover exponent). Those three critical exponents were obtained numerically confirming the scaling law. In addition, using the transformation  $I_{rms} \rightarrow I_{rms}/\epsilon^\alpha$  and  $n \rightarrow n/\epsilon^z$  the scaling invariance is shown in the chaotic sea, and this is a good indicative that the system is passing through a phase transition. The second method is an analytical one, using the solution of the diffusion equation. The comparison of these two descriptions is approached at the end of Sect. 5, where we can see a good agreement between the two formalisms. At the end, we confirm the phase transition replying the four questions proposed in Ref. [27]. First, broken symmetry is given at the phase space with  $\epsilon$  near the transition from integrability ( $\epsilon = 0$ ) to non-integrability ( $\epsilon \neq 0$ ). Second, the order parameter is identified as  $I_{rms,sat} \propto \epsilon^{\frac{1}{\gamma+1}}$ , since  $I_{rms,sat} \rightarrow 0$  when  $\epsilon \rightarrow 0$ . In addition, the susceptibility  $\chi \rightarrow \infty$  in the limit of  $\epsilon \rightarrow 0$ , this is a clear signature that the system is facing a continuous phase transition. Third, the elementary excitations are defined by the nonlinear function  $\epsilon \sin(\theta_n)$ , that leads to a random behaviour of the dynamics in the limit of small values of  $I$ , bringing chaotic orbits to the phase space. And finally fourth, the topological defects that impact on the particles diffusion are due to the regular structures present in the phase space. A chaotic orbit evolving near a periodic island suffers from the stickiness effect, harming the distribution of the particles. These factors allow us to conclude that the phase transition from integrability to non-integrability is a second-order phase transition.

**Acknowledgements** LKAM thanks FAPESP (2020/10602-1). CMK thanks to CAPES for support. YHH thanks CNPq. AKPF acknowledges FAPESP (2020/07219-1). JAO thanks FAPESP (Grant no. 2018/14685-9) and CNPq (Grant nos.

303242/2018-3, 421254/2016-5). EDL acknowledges support from CNPq (301318/2019-0) and FAPESP (2019/14038-6). CAPES, CNPq, and FAPESP are Brazilian agencies.

## Author contribution statement

Each author contributed equally to the paper.

## References

1. E.D. Leonel, *Invariância de escala em sistemas dinâmicos não lineares*, 1st edn. (Blucher, São Paulo, 2019)
2. N.A. Lemos, *Mecânica Analítica*, 2nd edn. (Livraria da Física, São Paulo, 2007)
3. H.A. Oliveira, *Revista Brasileira do Ensino de Física* (online) **36**, 1 (2014)
4. A.J. Lichtenberg, M.A. Lieberman, *Regular and Chaotic Dynamics*, 2nd edn. (Springer Science, New York, 1992)
5. B.V. Chirikov, *Phys. Rep.* **52**, 263 (1979)
6. J. Laskar, C. Froeschlé, A. Celletti, *Phys. D Nonlinear Phenom.* **56**, 253 (1992)
7. E. Piña, L.J. Lara, *Phys. D Nonlinear Phenom.* **26**, 369 (1987)
8. J.K.L. da Silva, D.G. Ladeira, E.D. Leonel, P.V.E. McClintock, S.O. Kamphorst, *Braz. J. Phys.* **36**, 700 (2006)
9. M.A. Lieberman, J.A. Lichtenberg, *Phys. Rev. A* **5**, 1852 (1971)
10. L.D. Pustynnikov, *Trans. Mosc. Math. Soc.* **2**, 1 (1978)
11. J.E. Howard, J. Humphreys, *Phys. D Nonlinear Phenom.* **80**, 256 (1995)
12. N. Fiedler-Ferrara, C.P.C. do Prado, *Caos: Uma introdução*, 1st edn. (Blucher, São Paulo, 1994)
13. S.H. Strogatz, *Nonlinear Dynamics and Chaos: With Applications to Physics, Biology, Chemistry and Engineering*, 2nd edn. (CRC Press, New York, 2018)
14. E.D. Leonel, J. Penalva, R.M.N. Teixeira, R.N.C. Filho, M.R. Silva, J.A. de Oliveira, *Phys. Lett. A* **379**, 1808 (2015)
15. J. Penalva, Master thesis (Univ Estadual Paulista, Rio Claro, 2014)
16. J.M. Greene, *J. Math. Phys.* **20**, 1183 (1979)
17. E.D. Leonel, P.V.E. McClintock, J.K.L. da Silva, *Phys. Rev. Lett.* **93**, 014101 (2004)
18. J.A. Mendéz-Bermúdez, R. Aguilar-Sanchez, *Phys. Rev. E* **85**, 056212 (2007)
19. D.G. Ladeira, J.K.L. da Silva, *J. Phys. A Math. Theor.* **40**, 11467 (2007)
20. D.G. Ladeira, J.K.L. da Silva, *Phys. Rev. E* **73**, 026201 (2006)
21. D.G. Ladeira, J.K.L. da Silva, *J. Phys. A Math. Theor.* **41**, 365101 (2008)
22. O.F.A. Bonfim, *Phys. Rev. E* **79**, 056212 (2009)
23. O.F.A. Bonfim, *Int. J. Bifurc. Chaos* **22**, 1250140 (2012)
24. D.F.M. Oliveira, M. Robnik, *Phys. Rev. E* **83**, 026202 (2011)
25. E.D. Leonel, *Math. Probl. Eng.* **2009**, 367921 (2009)

26. J.A. de Oliveira, R.A. Bizão, E.D. Leonel, Phys. Rev. E **81**, 046212 (2010)
27. J.P. Sethna, *Statistical Mechanics: Entropy, Order Parameters, and Complexity*, 2nd edn. (Oxford University Press, New York, 2020)
28. F. Reif, *Fundamentals of Statistical and Thermal Physics*, 1st edn. (Waveland Press, New York, 2009)
29. E.D. Leonel, C.M. Kuwana, M. Yoshida, J.A. de Oliveira, EPL (Europhysics Letters) **131**, 10004 (2020)
30. E. Butkov, *Mathematical Physics*, 1st edn. (Addison-Wesley, Reading, 1968)
31. C.M. Kuwana, Master thesis (Univ Estadual Paulista, Rio Claro, 2018)
32. T.S. Krüger, Doctoral thesis (Univ Federal do Paraná 2016)
33. E.D. Leonel, C.M. Kuwana, J. Stat. Phys. **170**, 69 (2018)